(Received 23 April 2025, Accepted 16 June 2025, Scheduled 3 July 2025)

Design and Performance Evaluation of a Single-Layer Planar UWB Antenna for Omnidirectional Coverage of 5G IoT Devices

Inaganti Rama Koteswara Rao[1,*], Ramavathu Sambasiva Nayak[2], and Karumuri Rajasekhar[3]

[1] *Department of Electronics & Communication Engineering, Jawaharlal Nehru Technological University, Kakinada Andhra Pradesh, India*
[2] *Department of Electronics and Communication Engineering, Sri Vasavi Institute of Engineering and Technology Nandamuru, Pedana, Andhra Pradesh, India*
[3] *Department of Electronics & Communication Engineering, JNTUK University College of Engineering Kakinada Andhra Pradesh, India*

ABSTRACT: This paper presents the design and performance evaluation of a planar ultra-wideband (UWB) antenna employing an elliptical dipole structure, targeting comprehensive omnidirectional coverage within the 1–10 GHz frequency band for 5G Internet of Things (IoT) applications. The antenna, constructed on a cost-effective FR4 substrate, exhibits an impressive impedance bandwidth of 10 : 1 ($|S_{11}| \leq -10$ dB) and frequency-dependent gain ranging from 3 to 8 dBi. Its design features ensure minimal side lobe levels below -20 dB, contributing to enhanced signal integrity and reduced interference. Notably, the azimuthal plane radiation pattern maintains a remarkable 1 dB out-of-roundness, facilitating robust communication in diverse IoT environments. Extensive 3D radiation pattern measurements affirm the antenna's effectiveness in optimizing signal propagation and reliability across varying deployment scenarios. This study underscores the significance of the elliptical dipole configuration in advancing UWB technology, highlighting its potential for seamless integration into future 5G IoT networks.

1. INTRODUCTION

The emergence of the Internet of Things (IoT) has garnered significant attention as a breakthrough in data communication, facilitating seamless and automated device-to-device interaction, also referred to as machine communication network or cyber-physical integration [1–3]. Within the IoT framework, objects are endowed with computer-based logic, enabling centralised monitoring and control through cloud-based analytics. Wireless networks play a pivotal role in connecting remote objects, forming the backbone of this interconnected system. The IoT involves the digital representation of physical entities, facilitating seamless interaction with Information and Communications Technology (ICT) components across diverse network infrastructures, including local area networks (LANs), wide area networks (WANs), and cloud environments. It is often regarded as the convergence point between ICT and operational technology systems, with diverse applications spanning industrial IoT for factory process control to sensing applications like power grid management, Intelligent transportation systems, traffic monitoring, video surveillance, smart city development, localization services, e-health systems, and crowd sensing [4, 5].

Ultra-wideband (UWB) technology stands out for its diverse applications, providing rapid data transfer, minimal energy usage, and a simplified setup devoid of a carrier signal, making it highly accessible for deployment [6]. Its low power spectrum density allows coexistence with other communication systems. UWB's features, including high bandwidth for HD video streaming and resistance to interference, make it suitable for consumer applications, business, and military incorporating IoT uses like tracking and sensor data collection [7]. In comparison to other technologies, UWB stands out with its low device complexity and cost, resilience to jamming, good time domain resolution, and compatibility with various wireless services [8]. It helps alleviate spectrum exhaustion by enabling shared spectrum use without interfering with other systems [9]. With short-range indoor applications in mind, UWB's benefits shine, supporting tasks like peripheral connectivity and image transfer [10, 11]. While UWB technology finds applications across various domains, it is particularly well suited for indoor environments due to its high data rate and low interference characteristics. Despite its numerous advantages, signal blockage can occur around large metallic objects [12].

The main challenge associated with IoT devices lies in their constrained coverage capability [13], a difficulty greatly impacted by mismatch between the Transmitter (Tx) and Receiver (Rx) antennas [14, 15]. In typical scenarios, Tx is often situated on ceilings or supporting walls. Conversely, IoT sensor nodes, with their flexibility in positions and orientations, may be located on the floor, table, or smart devices, as depicted in Fig. 1. The IoT nodes, encompassing medical devices, ecological detectors, toys, and microbots depend on signal coverage rather than power transfer. In indoor setups, the data transfer system must uniformly encompass a three-dimensional spherical region to account for sensor incongruence. Hence, a robust Rx

* Corresponding author: Inaganti Rama Koteswara Rao (irkrao1@gmail.com).

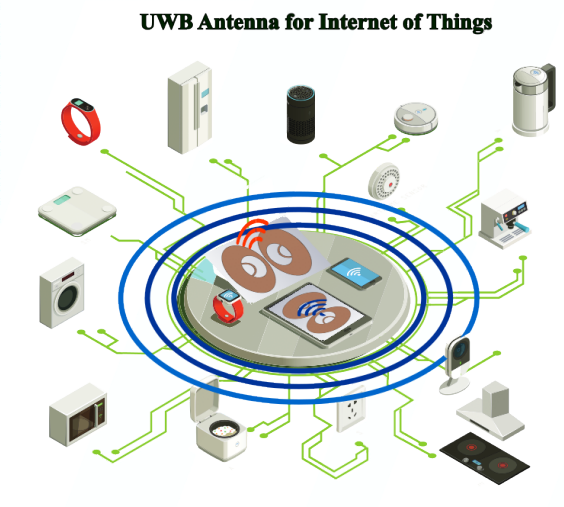

FIGURE 1. Smart home based different IoT applications.

system ensuring signal coverage at the sensor node, irrespective of its orientation, becomes essential [16]. High-performing Rx system with a uniformly covered three-dimensional (3D) spherical area is imperative to attain this objective. Traditional antenna choices such as dipole [17] and monopole [18] are considered optimal for azimuth coverage [19, 20]. However, their limited bandwidth and altitude plane coverage render them unsuitable for meeting the coverage requirements. In future IoT scenarios, where devices may operate across diverse frequency bands, opting for antenna designs that incorporate UWB technology and exhibit omnidirectional characteristics is advisable for optimal performance.

Several UWB antenna designs have been documented in the literature, showcasing a diverse range of applications [21]. For example, Mustaqim et al. engineered a rectangular UWB antenna specifically designed for wearable IoTs, with functionality spanning the 2.9 to 11 GHz band [22]. Saha et al. crafted a coplanar waveguide (CPW)-feed antenna, exhibiting substantial gain and covering the expansive 3.2 to 30 GHz range, catering to IoT applications [23]. Wang et al. introduced a flexible UWB antenna achieved through surface modification and self-metallization on a polyimide, offering coverage from 1.35 to 16.4 GHz [24]. Fang et al. innovated a compact UWB antenna based on a graphene-assembled film, tailored for wearables and spanning the 4.1–8 GHz range [25]. Di Natale and Giampaolo designed a reconfigurable UWB antenna specifically for wireless body area networks [26]. Zhang et al. designed a flexible UWB antenna adaptable to both flat and bent states, providing extensive coverage from 3.06 to 13.58 GHz [27]. El Gharbi et al. developed a UWB antenna with an operational range from 3.1 to 11.3 GHz [28]. The need for UWB antennas with stable omnidirectional radiation patterns in 5G IoT applications poses challenges related to bandwidth and efficient radiation. This research addresses these issues by proposing a planar elliptical dipole UWB antenna with slots, designed to enhance radiation pattern stability, providing a solution suited for UWB communication in IoT and 5G environments. The proposed antenna operates within the 1–10 GHz frequency range and is constructed on a cost-effective substrate. By leveraging a compact size and omnidirectional radiation characteristics, the antenna provides extensive connectivity in varied and dynamic IoT environments, ensuring seamless integration with future IoT devices and systems.

To address identified gaps, this study focuses on the necessity for a UWB antenna offering omnidirectional coverage that seamlessly integrates with current transceiver circuits. The proposed solution introduces a single-layer UWB antenna fabricated on an FR4 substrate, featuring compact dimensions of $116 \times 93 \times 1\,\text{mm}^3$. Notable attributes include the antenna's capacity for omnidirectional radiation along with UWB capabilities.

2. ANTENNA DESCRIPTION AND DESIGN PARAMETER IMPACTS

In the design of a planar elliptical antenna, the semi-major axis length ($\frac{W}{2}$) and semi-minor axis length ($\frac{L1+L2+L3}{2}$) are determined based on the substrate characteristics, including relative permittivity (ϵ_r) and substrate thickness (h). Assuming that the antenna is placed on a substrate with thickness h and relative permittivity ϵ_r and considering that the semi-major axis is aligned with the antenna width (W), the effective dielectric constant is computed as:

$$\epsilon_{\text{eff}} = \frac{\epsilon_r + 1}{2} + \frac{\epsilon_r - 1}{2}\left(1 + \frac{10h}{W}\right)^{-1/2} \tag{1}$$

The guided wavelength in the substrate, λ_g, is approximated based on the effective permittivity:

$$\lambda_g = \frac{\lambda_0}{\sqrt{\epsilon_{\text{eff}}}} = \frac{c}{f\sqrt{\epsilon_{\text{eff}}}} \tag{2}$$

Here, λ_0 is the free-space wavelength, c the speed of light, and f the operating frequency. Rearranging this expression allows estimating the semi-major axis $\left(\frac{W}{2}\right)$ as a function of the substrate parameters:

$$\frac{W}{2} \approx \frac{\lambda_g\sqrt{\pi}}{2} \tag{3}$$

This equation provides a geometrical approximation for designing the semi-major axis length of the elliptical antenna based on the effective guided wavelength.

For the semi-minor axis length $\left(\frac{L1+L2+L3}{2}\right)$, it can be expressed using an aspect ratio AR defined as the ratio between semi-minor and semi-major axes:

$$\frac{L1 + L2 + L3}{2} = AR \times \frac{W}{2} \tag{4}$$

Substituting from the expression for $\frac{W}{2}$:

$$\frac{L1 + L2 + L3}{2} = AR \times \frac{\lambda_g\sqrt{\pi}}{2} \tag{5}$$

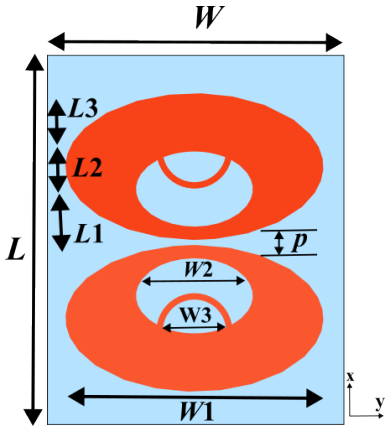

FIGURE 2. Schematic of the proposed UWB antenna.

The inner half-ellipse with major axis W3 functions as a capacitive slot that alters the current distribution near the feed region. This structure introduces reactive loading which facilitates broadband impedance matching. Furthermore, its geometry helps maintain azimuthal symmetry in the radiation pattern by stabilizing current flow at higher frequencies. The proposed antenna is illustrated in Fig. 2. The structure is located in the xy-plane, with the normal to the antenna surface along the z-axis. The geometry is symmetric about the yz-plane. Antenna performance metrics such as gain and reflection coefficient are influenced by its geometrical dimensions. The inner and outer slot dimensions are optimized using CST Microwave Studio. The antenna is fabricated on an FR4 substrate of 1 mm thickness with other optimized dimensions: $L = 116\,\text{mm}$, $W = 93\,\text{mm}$, $L1 = 23.68\,\text{mm}$, $L2 = 10.24\,\text{mm}$, $L3 = 13.24\,\text{mm}$, $W1 = 81.39\,\text{mm}$, $W2 = 36.87\,\text{mm}$, $W3 = 13.25\,\text{mm}$, and $p = 1.64\,\text{mm}$.

The proposed planar UWB antenna is engineered to deliver stable omnidirectional radiation and broad impedance matching across an extensive frequency range, targeting compact and cost-effective solutions for UWB communication systems, particularly in IoT applications. The design integrates an outer exponential dipole structure with inner circular and elliptical slot features to optimize electromagnetic performance. The antenna is excited via an SMA connector with a carefully optimized feed gap to ensure efficient power transfer and impedance matching. At lower frequencies, the antenna exhibits dipole-like radiation characteristics despite its compact profile, while at higher frequencies, the exponential slot geometry significantly contributes to gain enhancement and bandwidth extension. A key aspect of the design strategy is the incorporation of slots within the dipole arms, which serves to introduce reactive loading that improves impedance bandwidth and radiation stability. The inner circular slots primarily govern the reflection coefficient by modulating the local current distribution, whereas the elliptical slot dimensions and their offset position influence the gain performance, particularly at higher operating frequencies. The elliptical dipole geometry was chosen to balance compactness with improved radiation characteristics, enabling the antenna to meet the stringent requirements of modern UWB systems while maintaining structural simplicity and fabrication efficiency.

In the far-field region ($r \gg \lambda$), the radiated electric field magnitude from the elliptical antenna is approximately given by:

$$|\vec{E}(\theta,\phi)| \approx \frac{\eta I_0 k}{4\pi r} \cdot e^{jkr} \cdot F(\theta) \tag{6}$$

Here, η is the intrinsic impedance of the medium, I_0 the current amplitude, $k = \frac{2\pi}{\lambda}$ the wavenumber, and $F(\theta)$ the angular shaping function of the radiation pattern. The function $F(\theta)$ is defined as:

$$F(\theta) = \sin\theta \cdot \sqrt{\left(\frac{b}{a}\right)^2 \cos^2\theta + \sin^2\theta} \tag{7}$$

In this expression, a and b denote the semi-major and semi-minor axes of the elliptical structure, respectively. This angular function approximates the elevation-plane radiation characteristics of the antenna. The function $F(\theta)$ is introduced to model the directional variation based on ellipticity and is valid as an approximate shaping term.

3. SIMULATED AND MEASURED RESULTS

The planar elliptical dipole UWB antenna was fabricated using printed circuit board (PCB) technology, and experimental measurements were conducted in a controlled 3D anechoic chamber, as shown in Fig. 3. The reflection coefficient (S_{11}) and gain characteristics of the antenna are illustrated in Fig. 4. The results confirm that the UWB antenna operates effectively within the frequency range of 1 to 10 GHz, exhibiting measured gains between 3 and 8 dBi. The antenna maintains a favorable impedance match with $S_{11} < -10\,\text{dB}$ across the most of its $10:1$ bandwidth, ensuring a reliable $50\,\Omega$ input impedance. Although a slight degradation to $-8\,\text{dB}$ is observed in a specific frequency segment, these values remain acceptable for UWB applications. In the proposed configuration, the electric field distribution on the surface of the radiating patches at various frequencies is depicted in Fig. 5. The analysis reveals that enhanced electric field induction within the radiators facilitates resonance at the target frequencies, thereby contributing to an expanded bandwidth for the antenna design.

The simulated and measured 3D radiation patterns at representative frequencies, as illustrated in Fig. 6, demonstrate strong agreement, confirming the reliability of the proposed antenna design. Up to approximately 5 GHz, the antenna exhibits nearly omnidirectional radiation characteristics, with azimuthal variations confined within 1 dB, as seen in Fig. 6 and Fig. 7. This ensures consistent coverage and reliable communication in dynamic multipath environments, which is crucial for IoT applications. At higher frequencies, such as 10 GHz, the radiation pattern shows moderate degradation in omnidirectionality, primarily due to the increased electrical size of the structure and the excitation of higher-order modes. This results in the emergence of side lobes and a slight reduction in main lobe gain, with azimuthal variation extending to approximately 1.5 dB. Although the radiation pattern bandwidth is narrower than the impedance bandwidth, the antenna maintains stable performance across the operational band, offering a

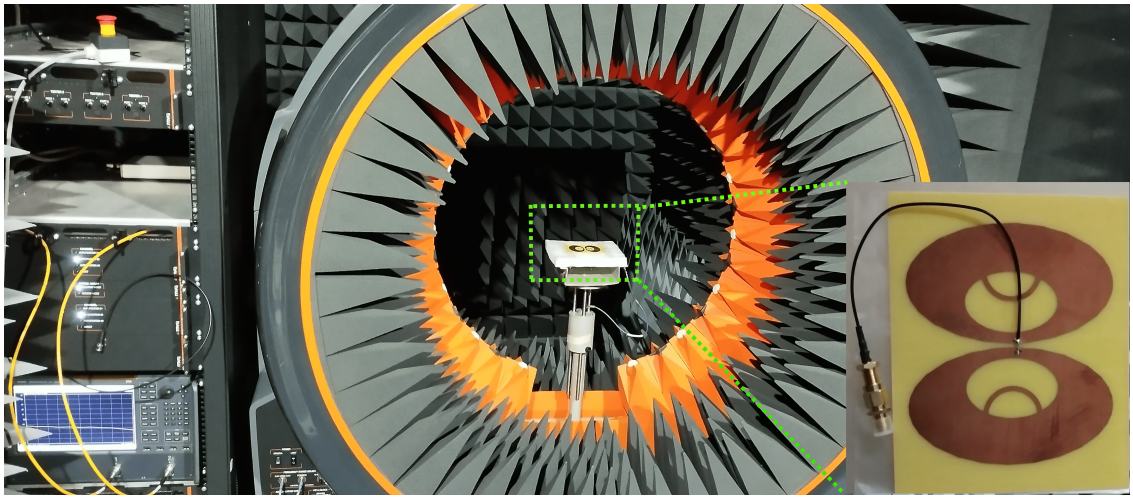

FIGURE 3. (a) An experimental setup with a fabricated prototype of the UWB antenna.

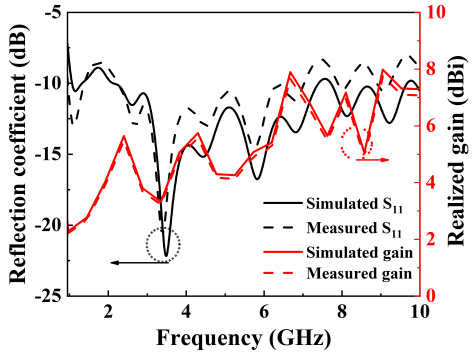

FIGURE 4. Simulated and measured reflection coefficients and gains for the proposed antenna.

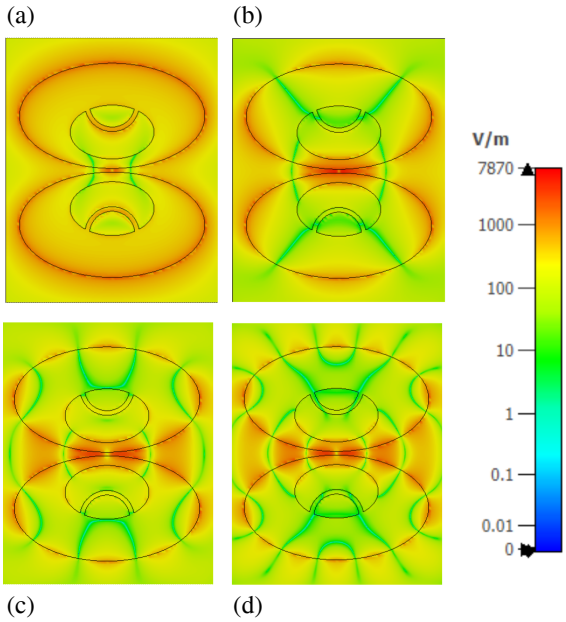

FIGURE 5. Simulated $\vec{E}$ field distribution (a) 1 GHz, (b) 4 GHz, (c) 7 GHz, and (d) 10 GHz.

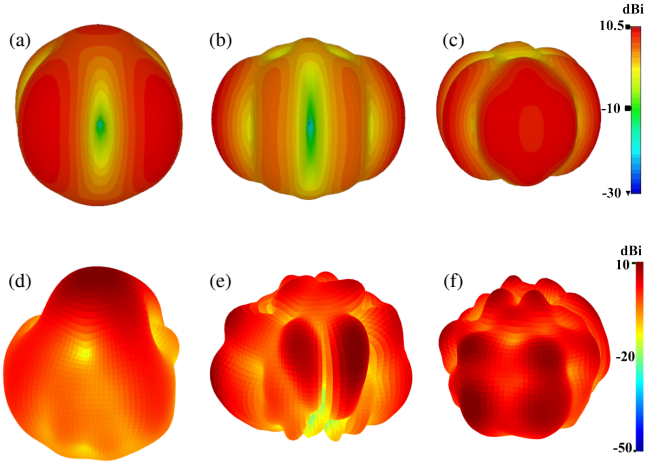

FIGURE 6. Simulated and measured 3D radiation patterns at 1 GHz (a) & (d), 5 GHz (b) & (e), and 10 GHz (c) & (f).

balanced trade-off among compactness, coverage consistency, and high-frequency efficiency. Fig. 7 illustrates the radiation patterns of the UWB antenna at frequencies of 1 GHz, 5 GHz, and 10 GHz, respectively. Within the 1–5 GHz range, the antenna exhibits nearly omnidirectional behavior in the elevation plane, characterized by two symmetrical lobes in the azimuthal plane. At frequencies exceeding 10 GHz, side lobes emerge in both the elevation and azimuthal planes, resulting in a gradual decrease in main lobe gain. The radiation efficiency of the proposed antenna varies between 70% and 80% across the 1–10 GHz frequency range, as shown in Fig. 8. The proposed antenna is distinguished by its easy integrability, compact, and cost-effective design, which facilitates straightforward fabrication while showcasing unique radiation characteristics. A comparative analysis of the proposed antenna's performance against previously reported UWB designs is presented in Table 1. This comparison highlights the advantages of the proposed antenna, affirming its contributions to the field of UWB technology and its potential applicability in future IoT systems.

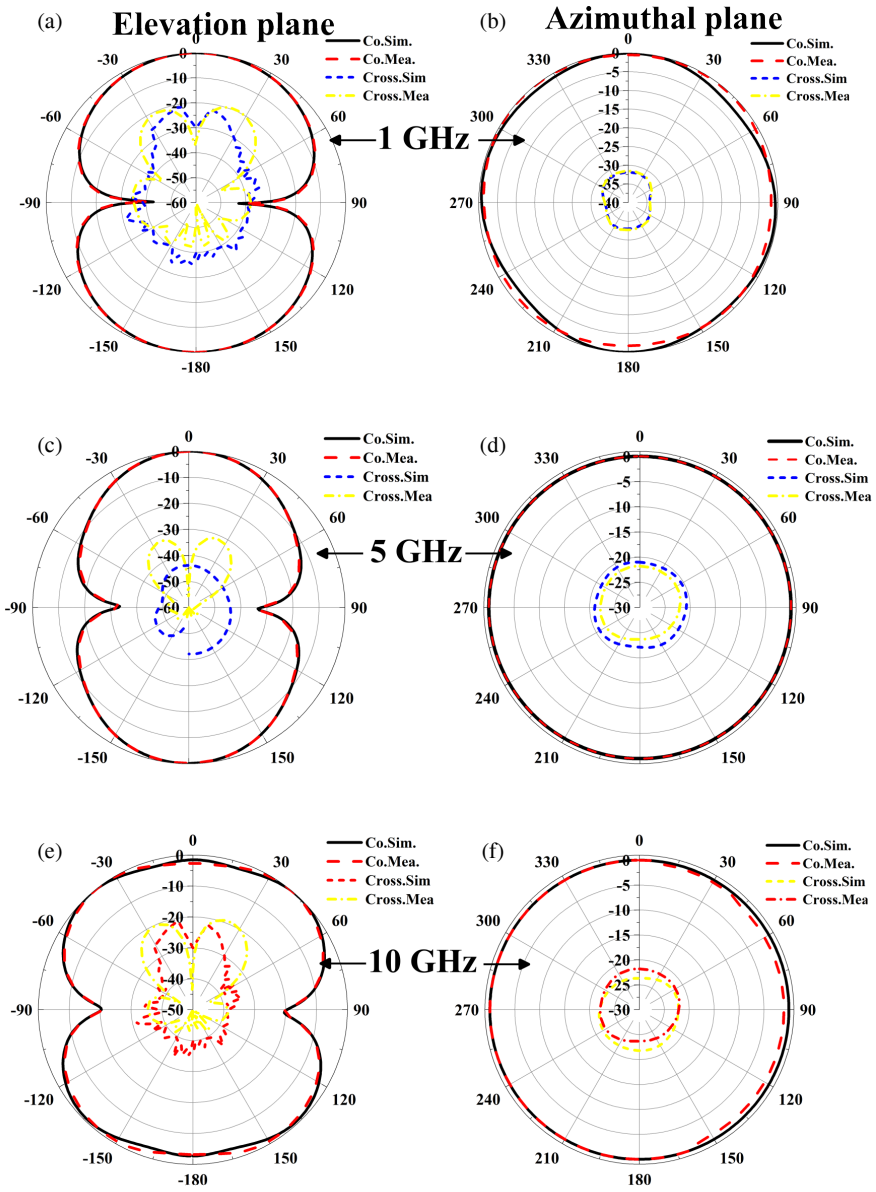

FIGURE 7. Radiation patterns at 1 GHz, 5 GHz, and 10 GHz.

TABLE 1. Comparison of the proposed antenna with the reported works.

Reference	Dimensions (λ_0)	Structure	Material	No. of Layers	Peak Gain (dBi)	Radiation Efficiency (%)	Bandwidth (GHz)
[30]	$0.5\lambda_0 \times 0.5\lambda_0 \times 0.38\lambda_0$	Shared-aperture	F4BME220	Multi	7.8 and 14	75	1.5–5, 25–29.3
[31]	$0.55\lambda_0 \times 0.67\lambda_0 \times 0.03\lambda_0$	Circular with slots	PF4-foam	Single	7.2	73	2.4–2.5, 4.6–10.1
[32]	$0.2\lambda_0 \times 0.2\lambda_0 \times 0.167\lambda_0$	Bowtie	Rogers RO4003C	Multi	–	80	1–6
[33]	$0.129\lambda_0 \times 0.258\lambda_0 \times 0.01\lambda_0$	Ribbon-Shaped Slot	FR-4	Single	4.12	80	3.1–10.8
[34]	$0.58\lambda_0 \times 0.87\lambda_0 \times 0.025\lambda_0$	Circular with slots	Rogers RO4350B	Multi	4	90	5.8–10
This work	$0.38\lambda_0 \times 0.31\lambda_0 \times 0.01\lambda_0$	Elliptical	FR4	Single	3 to 8	70–80	1–10

Note: All dimensions are normalized with respect to λ_0, which is the free-space wavelength at the lowest operating frequency of the antenna.

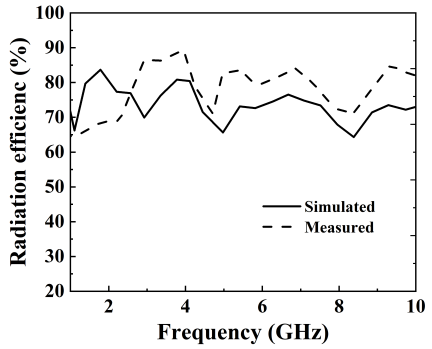

FIGURE 8. Radiation efficiency of the proposed antenna.

4. CONCLUSION

This paper has presented the design and performance evaluation of a planar elliptical dipole UWB antenna optimized for 5G IoT applications. The antenna achieved a wide impedance bandwidth from 1 to 10 GHz, maintaining consistent omnidirectional radiation patterns. Both simulated and measured results validated its suitability for reliable IoT device coverage, offering an impedance bandwidth ratio of 10 : 1, gain values ranging from 3 to 8 dBi, and side lobe levels below −20 dB. The compact form factor, ease of integration, and low fabrication cost support its practical deployment in modern IoT systems. To further enhance real-world applicability, radiation efficiency in multipath environments is improved through the integration of metamaterial-based ground structures and reconfigurable elements. These enhancements, along with extended performance at higher frequency bands, ensure the antenna's capability to meet the evolving demands of 5G and beyond IoT applications.

REFERENCES

[1] Hasan, Y. M., A. S. Abdullah, and F. M. Alnahwi, "UWB filtenna with reconfigurable and sharp dual-band notches for underlay cognitive radio applications," *Progress In Electromagnetics Research C*, Vol. 120, 45–60, 2022.

[2] Hasan, Y. M., "A compact monopole slotted patch-antenna for UWB applications," *Progress In Electromagnetics Research C*, Vol. 151, 65–71, 2025.

[3] Hasan, Y. M., K. D. Rahi, and A. A. Mahmood, "Rectangular antenna with dual-notch band characteristics for UWB applications," in *AIP Conference Proceedings*, Vol. 2591, No. 1, 020032, 2023.

[4] Hasan, Y. M., Z.-A. S. A. Rahman, and Y. Al-Yasir, "A miniature hexa-band antenna for internet of things applications using six quarter-wavelength resonators," *Advanced Electromagnetics*, Vol. 14, No. 1, 52–58, 2025.

[5] Hasan, Y. M., A. S. Abdullah, and F. Alnahwi, "Three-modes, reconfigurable filtenna system with UWB, WiMAX, and WLAN states for cognitive radio applications," *International Journal on Communications Antenna and Propagation (IRECAP)*, Vol. 14, No. 1, 15–23, 2024.

[6] Niemelä, V., J. Haapola, M. Hämäläinen, and J. Iinatti, "An ultra wideband survey: Global regulations and impulse radio research based on standards," *IEEE Communications Surveys & Tutorials*, Vol. 19, No. 2, 874–890, 2017.

[7] Rao, M. V., A. M. Ismail, M. N. M. Yasin, S. K. Noor, M. N. Osman, N. Rahman, J. Malik, and S. Yuvaraj, "Novel switched mode OAM beam generation using series-fed UCA antenna for AAVs nouvelle génération de faisceau MAO en mode commutéà l'aide d'une antenne UCA alimentée en série pour les AAVs," *IEEE Canadian Journal of Electrical and Computer Engineering*, Vol. 48, No. 2, 60–65, 2025.

[8] Almizan, H., M. H. Jwair, Y. A. Naiemy, Z. A. A. Hassain, L. Nagy, and T. A. Elwi, "Novel metasurface based microstrip antenna design for gain enhancement RF harvesting," *Infocommunications Journal*, Vol. 15, No. 1, 2–8, 2023.

[9] Nurhayati, N., F. Y. Zulkifli, E. Setijadi, B. E. Sukoco, M. N. M. Yasin, and A. M. D. Oliveira, "Bandwidth, gain improvement, and notched-band frequency of SWB Wave Coplanar Vivaldi antenna using CSRR," *IEEE Access*, Vol. 12, 16 926–16 938, 2024.

[10] Srinubabu, M. and N. V. Rajasekhar, "A high-isolation and compact 4-port MIMO antenna for 5G-NR sub-6 GHz applications," *Arabian Journal for Science and Engineering*, 1–17, 2025.

[11] Srinubabu, M. and N. V. Rajasekhar, "Enhancing diversity and isolation performance for a four-port MIMO antenna in FR-1 5G frequency bands," *IETE Journal of Research*, Vol. 70, No. 8, 6711–6726, 2024.

[12] Čelan, V., I. Stančić, and J. Musić, "Ultra wideband assisted localization of semi-autonomous floor scrubber," *Journal of Communications Software and Systems*, Vol. 13, No. 2, 109–119, 2017.

[13] Shinohara, N., "History and innovation of wireless power transfer via microwaves," *IEEE Journal of Microwaves*, Vol. 1, No. 1, 218–228, 2021.

[14] Akkermans, J. A. G., M. C. V. Beurden, G. J. N. Doodeman, and H. J. Visser, "Analytical models for low-power rectenna design," *IEEE Antennas and Wireless Propagation Letters*, Vol. 4, 187–190, 2005.

[15] Pour, Z. A., L. Shafai, and B. Tabachnick, "A practical approach to locate offset reflector focal point and antenna misalignment using vectorial representation of far-field radiation patterns," *IEEE Transactions on Antennas and Propagation*, Vol. 62, No. 2, 991–996, 2014.

[16] Kumar, M., S. Kumar, and A. Sharma, "Dual-purpose planar radial-array of rectenna sensors for orientation estimation and RF-energy harvesting at IoT nodes," *IEEE Microwave and Wireless Components Letters*, Vol. 32, No. 3, 245–248, 2022.

[17] Lin, W. and R. W. Ziolkowski, "Electrically small, single-substrate Huygens dipole rectenna for ultracompact wireless power transfer applications," *IEEE Transactions on Antennas and Propagation*, Vol. 69, No. 2, 1130–1134, 2021.

[18] Shaw, T. and D. Mitra, "Wireless power transfer system based on magnetic dipole coupling with high permittivity metamaterials," *IEEE Antennas and Wireless Propagation Letters*, Vol. 18, No. 9, 1823–1827, 2019.

[19] Rao, M. V., Y. B. Modugu, D. Mondal, S. Yuvaraj, and M. V. Kartikeyan, "Generation of dual-band OAM beam using planar uniform circular array for vehicular communications," *Microwave and Optical Technology Letters*, Vol. 66, No. 1, e13717, 2024.

[20] Sudheep, V., M. Srinivas, G. K. Kumar, M. V. Rao, S. Yuvaraj, and M. V. Kartikeyan, "A low-profile uca antenna to generate conical beam based on oam technique for vehicular applications," in *2023 3rd International conference on Artificial Intelligence and Signal Processing (AISP)*, 1–4, Vijayawada, India, March 2023.

[21] Zhang, Y., S. Li, Z.-Q. Yang, X.-Y. Qu, and W.-H. Zong, "A coplanar waveguide-fed flexible antenna for ultra-wideband

applications," *International Journal of RF and Microwave Computer-Aided Engineering*, Vol. 30, No. 8, e22258, 2020.

[22] Mustaqim, M., B. A. Khawaja, H. T. Chattha, K. Shafique, M. J. Zafar, and M. Jamil, "Ultra-wideband antenna for wearable Internet of Things devices and wireless body area network applications," *International Journal of Numerical Modelling: Electronic Networks, Devices and Fields*, Vol. 32, No. 6, e2590, 2019.

[23] Saha, T. K., T. N. Knaus, A. Khosla, and P. K. Sekhar, "A CPW-fed flexible UWB antenna for IoT applications," *Microsystem Technologies*, Vol. 28, No. 1, 5–11, 2022.

[24] Wang, Z., L. Qin, Q. Chen, W. Yang, and H. Qu, "Flexible UWB antenna fabricated on polyimide substrate by surface modification and in situ self-metallization technique," *Microelectronic Engineering*, Vol. 206, 12–16, 2019.

[25] Fang, R., R. Song, X. Zhao, Z. Wang, W. Qian, and D. He, "Compact and low-profile UWB antenna based on graphene-assembled films for wearable applications," *Sensors*, Vol. 20, No. 9, 2552, 2020.

[26] Di Natale, A. and E. D. Giampaolo, "A reconfigurable all-textile wearable UWB antenna," *Progress In Electromagnetics Research C*, Vol. 103, 31–43, 2020.

[27] Zhang, Y., S. Li, Z.-Q. Yang, X.-Y. Qu, and W.-H. Zong, "A coplanar waveguide-fed flexible antenna for ultra-wideband applications," *International Journal of RF and Microwave Computer-Aided Engineering*, Vol. 30, No. 8, e22258, 2020.

[28] El Gharbi, M., M. Martinez-Estrada, R. Fernández-García, S. Ahyoud, and I. Gil, "A novel ultra-wide band wearable antenna under different bending conditions for electronic-textile applications," *The Journal of the Textile Institute*, Vol. 112, No. 3, 437–443, 2021.

[29] Balanis, C. A., *Antenna Theory: Analysis and Design*, John Wiley & Sons, 2016.

[30] Cheng, Y. and Y. Dong, "Ultrawideband shared-aperture crossed tapered slot antenna for 5G applications," *IEEE Antennas and Wireless Propagation Letters*, Vol. 22, No. 3, 472–476, 2023.

[31] Samal, P. B., S. J. Chen, and C. Fumeaux, "Wearable textile multiband antenna for WBAN applications," *IEEE Transactions on Antennas and Propagation*, Vol. 71, No. 2, 1391–1402, 2023.

[32] Fiser, O., V. Hruby, J. Vrba, T. Drizdal, J. Tesarik, J. V. Jr, and D. Vrba, "UWB bowtie antenna for medical microwave imaging applications," *IEEE Transactions on Antennas and Propagation*, Vol. 70, No. 7, 5357–5372, 2022.

[33] Park, S. and K.-Y. Jung, "Novel compact UWB planar monopole antenna using a ribbon-shaped slot," *IEEE Access*, Vol. 10, 61 951–61 959, 2022.

[34] Mazzinghi, A., D. Barras, B. Danev, and A. Freni, "Miniaturized UWB dual-port antenna for localization applications," *IEEE Antennas and Wireless Propagation Letters*, Vol. 23, No. 3, 1080–1084, 2024.